Journal of Polymer Research (2023) 30:424
https://doi.org/10.1007/s10965-023-03805-4

ORIGINAL PAPER

# Synthesis of a single-component intumescent flame retardant and its high efficiency in imparting flame retardancy to polylactic acid

Nian Yin[1] · Yuhan Chen[1] · Yunfei Wang[1] · Shanjun Gao[1] · Chunhui Shen[1]

Received: 7 July 2023 / Accepted: 16 October 2023 / Published online: 30 October 2023


## Abstract

In this paper, a single-component intumescent flame retardant di-(3-aminopropyltriethoxysilane) spirocyclic pentaerythritol diphosphate (PDAP) was synthesized, imparting flame retardancy to polylactic acid (PLA), which using melt blending process. The chemical structure and thermal stability of PDAP were characterized by test methods such as Fourier transform infrared spectroscopy (FTIR) and thermogravimetric analysis (TGA). The fire retardancy of PLA/PDAP was evaluated by test methods such as limiting oxygen index (LOI) and vertical burning test (UL-94). The thermal stability of PLA/PDAP was studied by TGA and thermogravimetry-Fourier transform infrared spectrometry (TG-FTIR). According to the results of laser Raman spectroscopy (LRS) and FTIR, the possible flame retardant mechanism of PLA/PDAP was discussed. With only 20 wt% addition of PDAP, PLA/PDAP could achieve 11.98% char residues at 800 °C. The LOI value of PLA/PDAP achieved 37%, UL-94 test reached V-0 rating. And higher fireproof performance with 62.1% reduced peak heat release rate (PHRR), 36.8% reduced total heat release rate (THR) and 19.5% reduced average effective combustion heat (av-EHC) value than PLA. The results show that PDAP has remarkable flame retardant effect on PLA, which provides an excellent research case for flame retardant modification of PLA plastic products.

**Keywords** PLA composites · Flame retardant · Single-component · Synergistic effect

## Introduction

Polylactic acid (PLA) is a very important environmentally friendly, biodegradable polymer material [1]. PLA could be directly recycled and completely degraded to $CO_2$ and $H_2O$, which has the advantages of excellent biocompatibility and biodegradability, good processing performance and abundant supply of raw materials. Therefore, it could be applied in various fields, such as packaging materials, disposables, medical and health fields [2–4]. However, the structural characteristics and high carbon content of PLA result in PLA being not only extremely flammable, but also having severe melt-drops during combustion [5]. Due to PLA easily degrades at high temperatures, poses a major safety risk and greatly limits its application in electronics and various commercial fields [6]. Thus it is importance to promote the thermostability and fire retardancy of PLA. The incorporation of flame retardants into polymers by conventional thermoplastic processing has been widely used to enhance the flame retardancy of plastics, so the synthesis of flame retardants is the key to obtaining good flame retardancy [7].

Intumescent flame retardant (IFR) is an environmentally friendly flame retardant with high efficiency and low toxicity, which has been widely applied in PLA composites [8, 9]. The most prominent IFR systems are compounds containing phosphorus/nitrogen, where the addition of nitrogen reduces the addition of phosphorus-based flame retardants, and collectively contributes to the establishment of a stable charcoal layer [10]. Besides phosphorus and nitrogen elements, researchers have combined other elements (e.g. Si, Mg, Ca, etc.), showing various degrees of synergistic effects [11, 12].

A common method of preparing IFR systems is to synthesize single-component IFR [13, 14], which are chemically synthesized to make the "three sources in one" of IFR systems, such as polyol phosphates and triazine derivatives. Qi et al. [15] synthesized a new single-component IFR PSTBP, the residual amount of PSTBP achieved 34.58% at 800 °C. PP/PSTBP composite had a LOI of 32.5% at a PSTBP

✉ Shanjun Gao
sjgao@whut.edu.cn

[1] Department of Polymer Materials and Engineering, School of Material Science and Engineering, Wuhan University of Technology, Wuhan, People's Republic of China

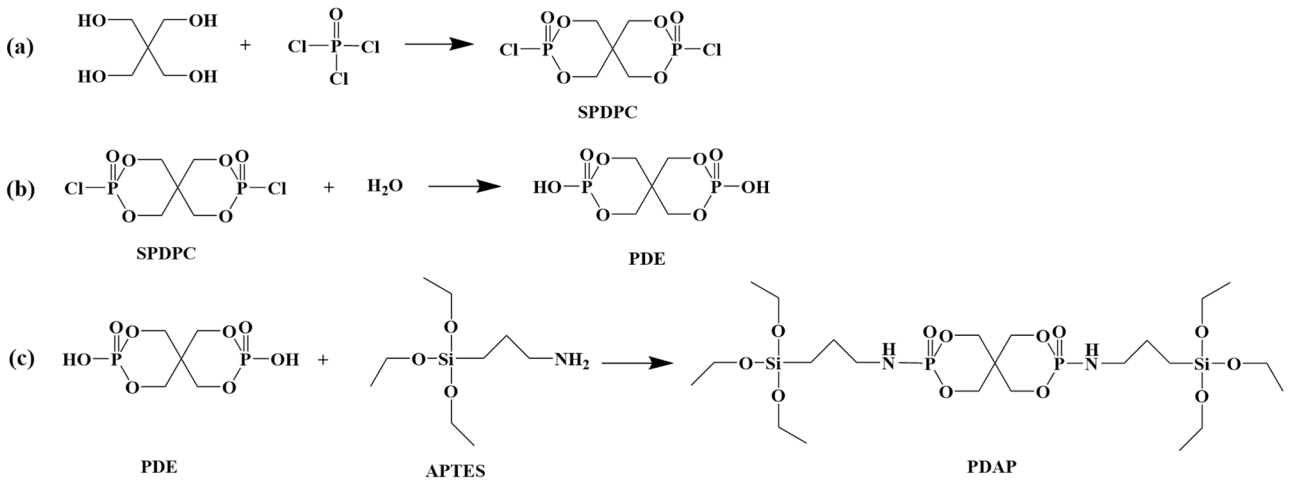


**Scheme 1** Synthetic route of PDAP

content of 30.0 wt%. Zhu et al. [16] synthesized a hyperbranched triazine-piperazine pyrophosphate HTPPP, when loaded at 25 wt% HTPPP, PP composites had an LOI of up to 30.5%, and UL-94 achieved V-0 rating, as well as initial decomposition temperature of HTPPP in air up to 275 °C. Lai et al. [17] synthesized a new IFR PETBP, and the test results showed that at 25 wt% PETBP, the PP/PETBP composite had a LOI of 29.5% with a V-0 rating for UL-94 testing. Recently, silicone-containing flame retardants possess good thermal stability and good compatibility. Li et al. [18] synthesized a new IFR (PSiNII) containing Si/P/N elements, and blended 20 wt% PSiNII into polypropylene, and the LOI value improved from 17.4 to 29.5%. Fang et al. [19] synthesized a new flame retardant (TDA) containing P/N/Si. The thermogravimetric analysis results showed that the cured EP retained excellent thermal stability after the introduction of TDA. When 25.0 wt% of TDA was added, the LOI value improved to 33.4% and UL-94 reached V-0 rating.

In this paper, IFR PDAP containing P/N/Si was synthesized from pentaerythritol, phosphorus oxychloride and 3-aminopropyltriethoxysilane and blended into PLA matrix. It is expected that P/N/Si will show excellent synergistic effects in PLA in the final product to achieve the excellent flame retardancy.

## Experimental

### Materials

Polylactic acid (PLA), Natureworks Company (US); phosphorus oxychloride ($POCl_3$, AR), Wuhan Geochemical Technology Co., Ltd (Wuhan China); pentaerythritol (PER), 3-aminopropyltriethoxysilane (APTES, AR), Aladdin (Shanghai, China); dichloromethane, anhydrous ethanol, acetonitrile, acetone (AR), Sinopharm (Shanghai, China). These materials were experimented with as they were purchased.

### Synthesis of flame retardant (PDAP)

The synthesis scheme of PDAP was carried out in three steps as shown in the synthetic route of Scheme 1.

#### Synthesis of spirocyclic pentaerythritol diphosphoryl chloride (SPDPC)

First, pentaerythritol 13.6 g (0.1 mol), phosphorous trichloride 28 ml (0.3 mol), and acetonitrile solution 100 mL were mixed into a 250 mL flask with a reflux condenser tube, thermometer, and an off-gas absorber, nitrogen was passed through the flask, stirred, and heated to 70 °C for 2 h. The temperature was raised to reflux temperature (85 °C) for 10 h, cooled down, then washed with anhydrous ethanol and dichloromethane, and placed in an oven to dry for 10 h. A white powder SPDPC was prepared with a yield of 12.3 g.

#### Synthesis of pentaerythritol diphosphate (PDE)

SPDPC 8 g (0.027 mol) suspended in acetonitrile solution 55 mL was placed in a 100 mL flask with a reflux condenser tube, thermometer and an off-gas absorber, stirred and heated to 80 °C in $N_2$. Then 6 mL of distilled water was slowly added dropwise, kept this temperature for 1.5 h. Cooled down and filtered, then washed by acetone and

acetonitrile, and placed in an oven to dry for 10 h to obtained a white powder PDE, the yield was 5.8 g.

### Synthesis of di-(3-aminopropyltriethoxysilane) spirocyclic pentaerythritol diphosphate (PDAP)

PDE 4.8 g (0.018 mol) was added into a 250 mL flask contained acetonitrile 50 mL, which equipped with reflux condenser tube, thermometer. Meanwhile, 3-aminopropyltriethoxysilane (APTES) 12 g (0.054 mol) dissolved in acetonitrile 30 mL, which was added dropwise to this container. Next slowly heated to 75 °C for 10 h. Cooled down, separated with centrifugal machine, washed twice with acetonitrile, and put in an oven for 24 h to obtained a white lumpy solid PDAP, the yield was 5.6 g.

### Preparation of PLA composites

Firstly, evenly mixing PDAP and PLA for later use, PLA/PDAP were prepared by melt blending method in a microcompactor with the relevant parameters of 50 rpm, 180 °C, and 15 min of compacting time, and then by hot press molding process at 180 °C and 8 MPa for 6 min. The specific composition formulations were listed in Table 1.

## Results and discussion

### Chemical structure characterization of PDAP

The FTIR spectra of PDAP, PDE, SPDPC and APTES (a raw material) were shown in Fig. 1, whose structures were characterized by FTIR. For SPDPC, the characteristic absorption bands of 547 $cm^{-1}$ (P-Cl), 855 $cm^{-1}$ (P-O), 1311 $cm^{-1}$ (P=O), and 1025 $cm^{-1}$ (P-O-C) proved the structure of SPDPC synthesized in the first step [20, 21]. In the FTIR spectra of PDE, the disappearance of the P-Cl (547 $cm^{-1}$) absorption band, while the appearance of the O-H (3477 $cm^{-1}$) absorption band illustrated the synthesis of PDE. As for PDAP, there was no absorption band at 547 $cm^{-1}$, the absorption bands of N-H stretching vibration, N-H bending vibration and Si-O-C could be observed at 3372, 1456 and 1088 $cm^{-1}$, respectively [22, 23]. When comparing the FTIR of APTES and PDAP, the symmetric vibrational bands of primary amine (-$NH_2$) at 3395 and 3326 $cm^{-1}$ were replaced by a vibrational single peak of secondary amine (-NH-) at 3372 $cm^{-1}$, which demonstrated that -$NH_2$ group reacted with P-OH group [24]. And three peaks at 1228 $cm^{-1}$ (P=O), 1025 $cm^{-1}$ (P-O-C) and 821 $cm^{-1}$ (P-O) still existed, as well as a new absorption band at 780 $cm^{-1}$ (P-N) [12], which showed the successful synthesis of PDAP. 2929 and 2879 $cm^{-1}$ was for the absorption bands of C-H ($CH_3$, $CH_2$) of APTES in the FTIR spectra.

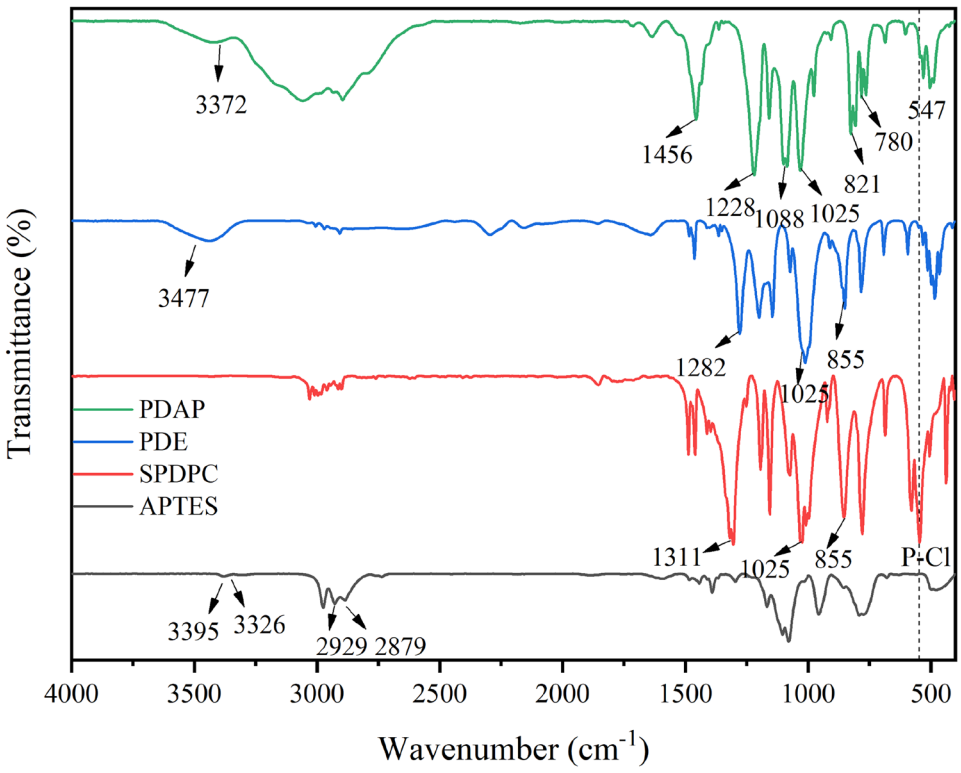


**Fig. 1** FTIR spectra of SPDPC, PDE, PDAP and APTES

In order to characterize the structure of the products, NMR spectrum was also used. The $^{1}$H NMR and $^{31}$P NMR spectrum of SPDPC and PDAP were shown in Fig. 2. As can be observed from the $^{1}$H NMR spectrum of SPDPC in Fig. 2(a), the solvent absorption peak at 4.73 ppm was for CAS deuterium oxide. The double peaks at 4.10 and 4.12 ppm were the absorption peaks corresponding to the H protons on the spiro ring structure [19]. The $^{1}$H NMR spectrum of PDAP showed that the solvent absorption peak of CAS deuterium oxide at 4.73 ppm, 1.14 ppm was the absorption peak of -Si-O-$CH_2$-$\boldsymbol{CH_3}$ (1), 3.68 ppm for Si-O-$\boldsymbol{CH_2}$-$CH_3$ (2) [25], 0.73 ppm for -Si-$\boldsymbol{CH_2}$-$CH_2$- (3), 1.75 ppm for -Si-$CH_2$-$\boldsymbol{CH_2}$- (4) [26], 2.68 ppm for -$CH_2$-$CH_2$-$\boldsymbol{CH_2}$- (5), 2.98 ppm for -$CH_2$-$\boldsymbol{NH}$-P- (6), and the double peaks of 4.16 and 4.18 ppm was the absorption peaks corresponding to the H proton on the spiro ring structure (7), which proved the molecular structure of PDAP. The $^{31}$P NMR spectrum of SPDPC was shown in Fig. 2(b), there was only one chemical environment of P-atom at -2.94 ppm. The $^{31}$P NMR spectrum of PDAP also had only one P-atom absorption peak at -2.39 ppm. indicating that PDAP has been synthesized successfully.

The results of PDAP elemental analysis data were shown in Table 2. The element analyzer determined the amount of six elements, O, C, N, H, Si, and P, in the PDAP samples as 35.94, 5.27, 33.92, 6.53, 10.36, and 7.98 wt%, respectively. The comparison showed that the actual and theoretical values of the content of different elements in PDAP were almost the same, illustrating that the structure of PDAP was as expected According to the above results, the conclusion that PDAP had been successfully synthesized could be drawn.

## Thermal stability of PDAP

Figure 3 showed the TGA and DTG curves of PDAP under nitrogen atmosphere from 35 to 800 °C. The decomposition of PDAP was a single step process under $N_2$ atmosphere, with a rapid weight loss between 200 and 450 °C. The $T_{5wt\%}$ and $T_{max}$ of PDAP were 176.54 and 365.92 °C, respectively. At 800 °C, the residual amount of PDAP was 49.74%, which indicated that PDAP had an excellent charring ability. The TGA and DTG results indicated that the decomposition of PDAP had mainly a large weight loss phase. It occurred between 250 and 450 °C and could be considered as the breakage of phosphate ester bonds, which would generate substances such as phosphoric acid to act in the subsequent flame retardant process and it would act to trap free radicals [15]. The TGA of PDAP between 600 and 800 °C showed a small weight loss, then a stable intumescent char layer was eventually formed.

## Flame retardancy of PLA composites

### LOI and UL-94 tests

For the purpose of evaluating its flammability, PLA and PLA/PDAP with various components were characterized by LOI and UL-94 tests presented in Table 1. The LOI value of PLA was only 20.1%, which failed the UL-94 test, belonged to flammable material and was prone to molten drops during the combustion process. When loaded with 5 wt%, 10 wt% and 15 wt% of PDAP to PLA matrix material, the LOI values were improved, but UL-94 results only achieved V-2 rating, so their flame retardant effect was not enough. The LOI values were as high as 37% and 37.4% when PDAP was added at 20 wt% and 25 wt% respectively, and the PLA/PDAP composites achieved V-0 rating, which showed that the flame retardant PLA self-extinguished rapidly without melt-drop phenomenon. Chen et al. [27], produced PLA flame-retardant composites from PLA and hyperbranched polyphosphate (HPE), the 20 wt% addition of HPE resulted in PLA composites with 35% LOI value and V-0 rating. Moreover, the combustion test results of PLA/ammonium polyphosphate (APP) were listed in the Supporting materials, and the results revealed that a better fire retardant effect of PDAP for PLA was achieved. PLA-4 and PLA-5 showed relatively similar LOI values. Both of them had achieved V-0 rating, compared to PLA-4 in which the amount of flame retardant added was lower and had fewer effects on other properties of the matrix material.

### CCT analysis

With a purpose to further assess the fire retardancy of PLA composites, combustion performance of the materials was measured by CCT, the results and related parameters were presented Fig. 4; Table 3.

In Fig. 4(a), it was observed that the heat release rate (HRR) graph of PLA presented a single peak, whereas the HRR curves of PLA-4 and PLA-5 in the samples with more PDAP addition showed two peaks, which was mainly due to the degradation in the composites and shielding barrier effect by the intumescent char layers. Secondly, these intumescent char layers were degraded further, which resulted in the degradation of the substrate material to generate a new intumescent char layer [28]. In Table 3, as PDAP was increased, the PHRR values of PLA/PDAP displayed a gradient decrease compared to pure PLA, and a slight decrease of PHRR values of PLA-2. The PHRR values of PLA-3, PLA-4 and PLA-5 were 387, 186 and 110 kW/m$^2$, respectively, which were reduced by 21.2%, 62.1% and 77.6%, respectively. The significant reduction in PHRR for PLA/PDAP could be explained in two aspects. On the one hand,

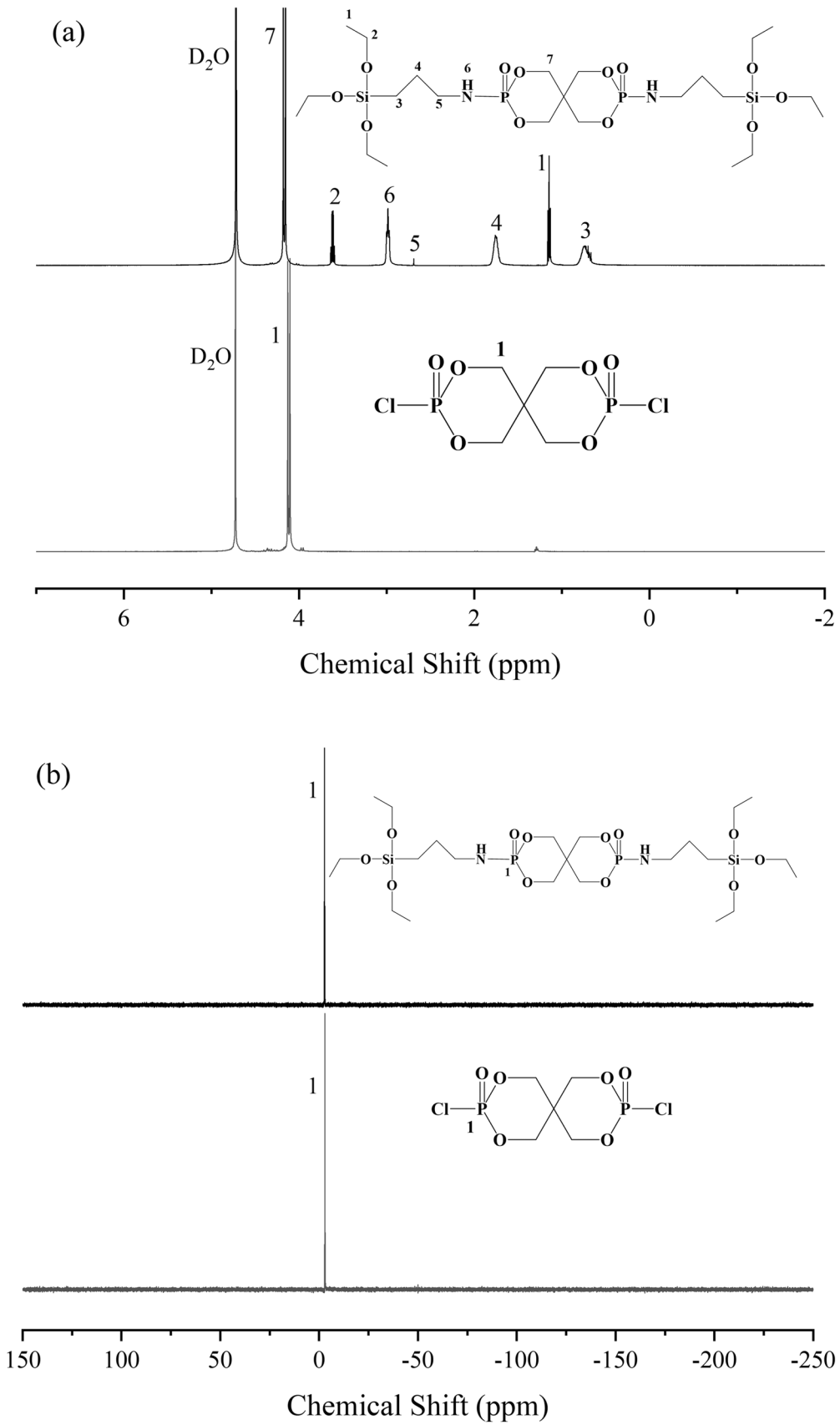


**Fig. 2** $^{1}$H NMR spectrum of SPDPC, PDAP (**a**) and $^{31}$P NMR spectrum of SPDPC, PDAP (**b**)

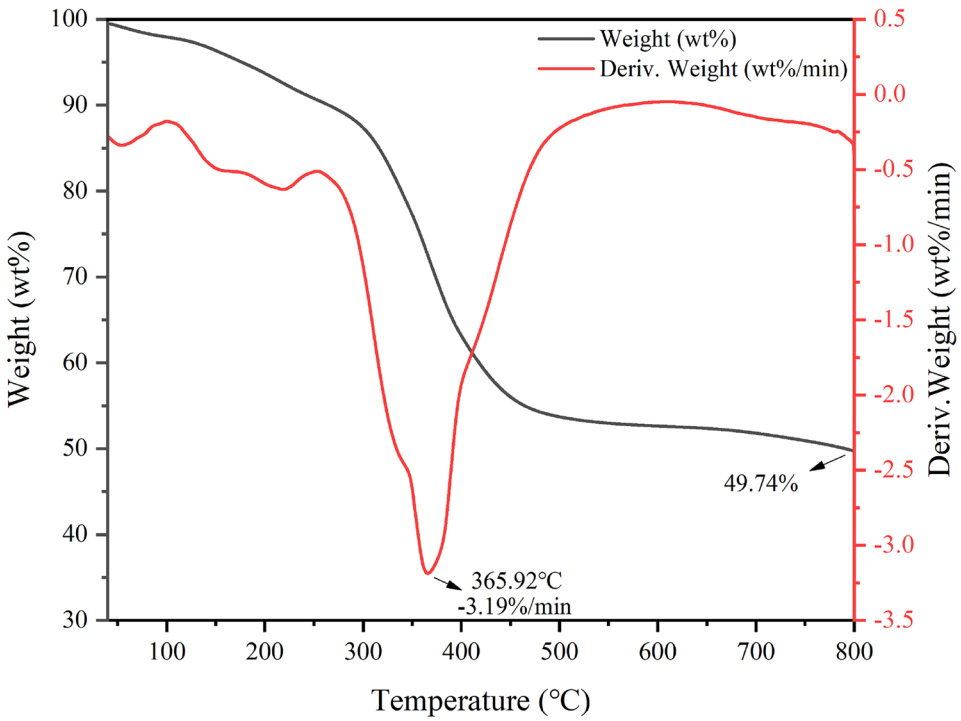


**Fig. 3** TGA and DTG curves of PDAP under $N_2$

**Table 1** Formulation of PLA composites and results for LOI and UL-94 test

| Sample | PLA (wt%) | PDAP (wt%) | LOI (%) | UL-94 vertical rating | |
|---|---|---|---|---|---|
| | | | | Rating | Dropping |
| PLA-0 | 100 | 0 | 20.1 | Failed | Yes |
| PLA-1 | 95 | 5 | 26 | V-2 | Yes |
| PLA-2 | 90 | 10 | 30.3 | V-2 | Yes |
| PLA-3 | 85 | 15 | 34 | V-2 | Yes |
| PLA-4 | 80 | 20 | 37 | V-0 | No |
| PLA-5 | 75 | 25 | 37.4 | V-0 | No |

PDAP was decomposed by a heat-absorbing reaction, which acted as a heat absorber and led to a lower temperature of the combustion system. Meanwhile, the water vapor and non-flammable gas released from PDAP decomposition would dilute the oxygen concentration around the material which would prevent it from burning fully. Moreover, the substances such as phosphate esters produced from the thermal degradation of PDAP covered the surface of the material to reduce more energy and mass exchange between two phases (condensed and gas phase), which prevented the matrix material from further combustion [29]. Besides the above reasons, the flame retardant element Si migrated to surface of the char layer and promoted production of the char layer. The THR of PLA-3, PLA-4 and PLA-5 was decreased by 9.6%, 36.8% and 48.2%, respectively, compared to 77.20 MJ/m2 for PLA-0. This meant that PDAP formed a dense and continuous char layer in matrix material, which could be a physical barrier that limited energy and mass exchange to protect substrate material. The Av-EHC represented the extent of volatile combustion for studying gas-phase flame retardant mechanism, where a decrease in this value indicated flame suppression or fuel dilution. The Av-EHC of PLA-4 and PLA-5 decreased to 17.646 and 17.480 MJ/kg, respectively, as shown in the table, which was 19.5% and 20.2% lower compared to PLA-0. This was mainly due to the flame suppression effect of the phosphorus compounds released by radical capture mechanism by trapping reactive radicals in the flame [10]. The Av-EHC for PLA-2 and PLA-3 with low flame retardant additions was only slightly reduced.

**Table 2** EA and XRFs data of PDAP

| | Element content (wt%) | | | | | |
|---|---|---|---|---|---|---|
| | C | H | N | O | P | Si |
| Theoretical value | 41.44 | 7.81 | 4.21 | 28.82 | 9.31 | 8.41 |
| Actual value | 35.94 | 5.27 | 6.53 | 33.92 | 10.36 | 7.98 |

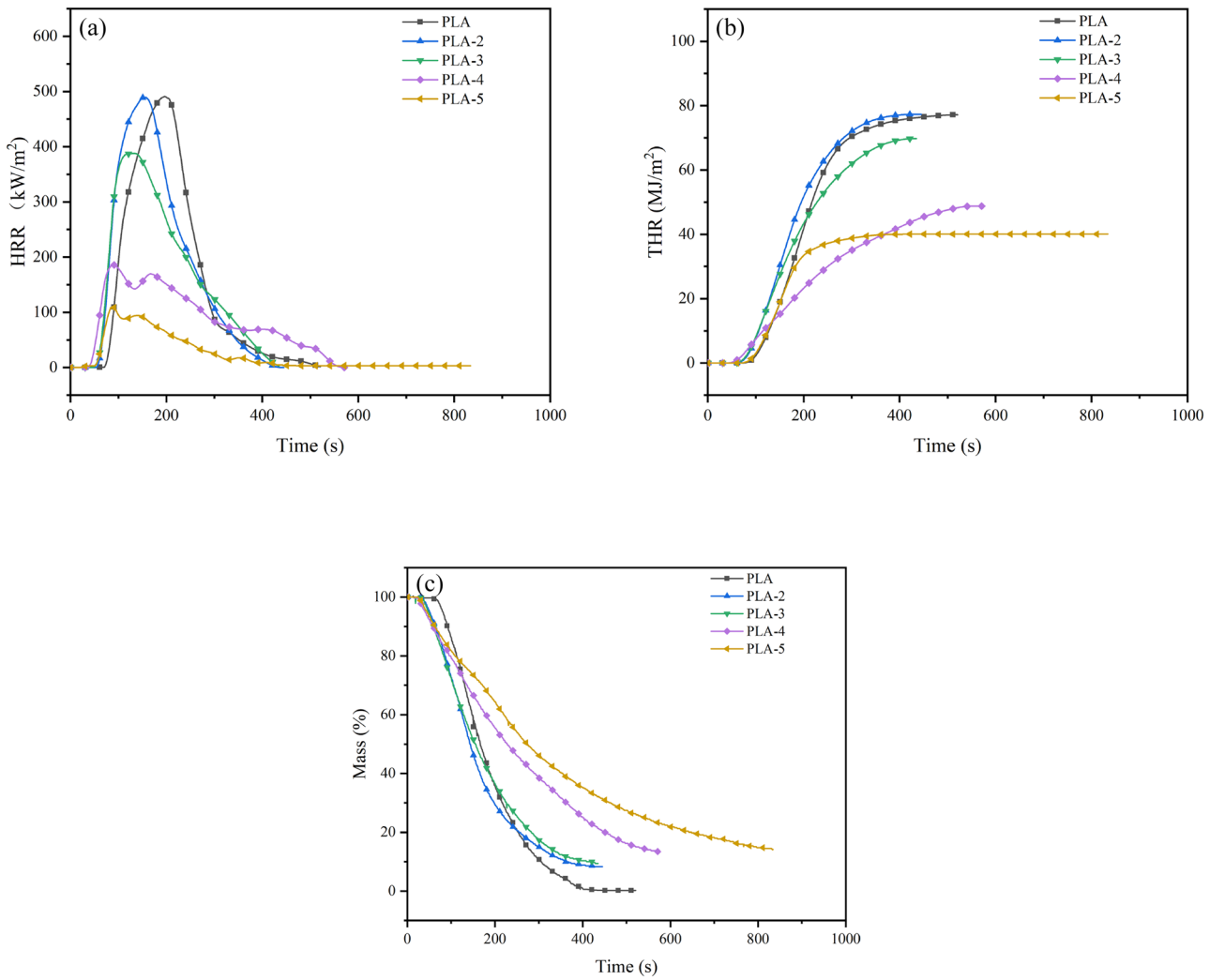


**Fig. 4** **a** HRR-time curve. **b** THR-time curve. **c** Mass-time curve. Note: pure PLA and PLA composites

The mass loss curve could demonstrate the role played by the fire retardant in the condensed phase. Pure PLA was basically residue-free after CCT test, and as PDAP was added, the residue of PLA/PDAP gradually increased. The residues of PLA-4 and PLA-5 reached 13.43% and 14.15%. Furthermore, the fire performance index (FPI), defined as the ratio of ignition time (TTI) to PHRR, from the table, it could be noticed that with the addition of PDAP, the FPI values became larger and larger, where PLA-4 and PLA-5 were significantly larger compared to PLA-0. This further verified that PDAP had a superior effect on PLA, consistent with the previous findings.

**Table 3** CCT data of PLA and PLA composites

| Sample | PHRR (kW/m$^2$) | THR (MJ/m$^2$) | $t_{PHRR}$ (s) | FPI (m$^2$s/kW) | Av-EHC (MJ/kg) | Residue (wt%) |
|---|---|---|---|---|---|---|
| PLA-0 | 491 | 77.20 | 196 | 0.043 | 21.909 | 0.19 |
| PLA-2 | 489 | 77.17 | 157 | 0.076 | 20.991 | 8.28 |
| PLA-3 | 387 | 69.78 | 134 | 0.088 | 20.524 | 9.39 |
| PLA-4 | 186 | 48.78 | 90 | 0.188 | 17.646 | 13.43 |
| PLA-5 | 110 | 40.00 | 88 | 0.309 | 17.480 | 14.15 |

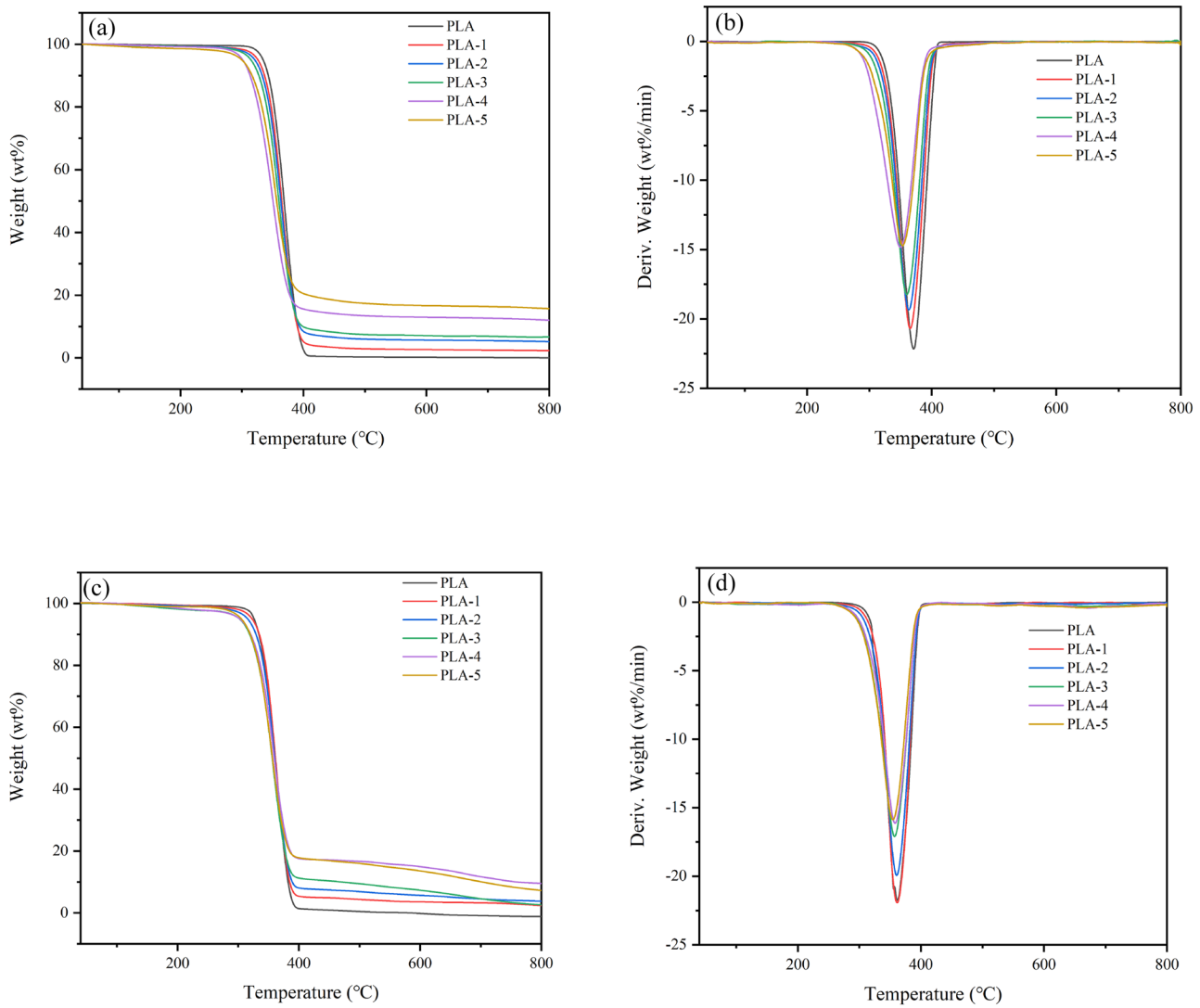


**Fig. 5** TGA and DTG curves of PLA and PLA/PDAP under $N_2$ and Air

## Thermal degradation of PLA composites

### TGA and DTG

As shown in Fig. 5 were the TG and DTG curves of pure PLA and PLA/PDAP in the presence of $N_2$ and air atmosphere, where the relevant data under $N_2$ atmosphere were shown in Table 4. Only one thermal decomposition stage was observed for PLA and PLA/PDAP under $N_2$. The $T_{5wt\%}$ of PLA was 334.42 °C, $T_{max}$ was 371.17 °C, and the char residue at 800 °C was 0.02 wt%. When PDAP was added to PLA, the initial degradation temperatures of PLA/PDAP composites were all earlier than PLA, which was supposed to be because of the lower decomposition temperature of

**Table 4** Relevant parameters of TGA and DTG for PLA and PLA/PDAP under $N_2$

| Sample | $T_{5wt\%}$ (°) | $T_{20wt\%}$ (°C) | $T_{50wt\%}$ (°C) | $T_{max}$ (°C) | $R_{max}$ (wt%/min) | Residue at 800 °C (%) |
|---|---|---|---|---|---|---|
| PLA-0 | 334.42 | 352.27 | 368.45 | 371.17 | 22.16 | 0.02 |
| PLA-1 | 325.93 | 347.52 | 364.83 | 365.45 | 20.68 | 2.29 |
| PLA-2 | 320.84 | 344.62 | 363.08 | 363.28 | 19.34 | 5.16 |
| PLA-3 | 314.42 | 340.25 | 360.02 | 360.11 | 18.24 | 6.64 |
| PLA-4 | 301.22 | 332.52 | 356.44 | 349.69 | 14.83 | 11.98 |
| PLA-5 | 299.82 | 326.73 | 350.41 | 353.24 | 14.72 | 15.67 |

PDAP, decomposing at an early stage to form a stable char that could be a barrier to protect the underlayer material from more degradation [6]. The $T_{max}$ of all samples did not vary significantly, but the maximum degradation rate decreased markedly with increasing PDAP additions. The final char residue of PLA/PDAP composites were higher than that of pure PLA, probably because silicones had lower surface energy and migrated to the polymer surface at high temperature to form a surface layer containing silicon, which prevented further decomposition of the polymer. Thus there was a significant increase in the residual char rate of the system [25]. At 20 wt% and 25 wt% PDAP additions, the PLA/PDAP composites showed residual char at 800 °C as high as 11.98% and 15.67%. The char layer formed by PLA-4 and PLA-5 had better thermal stability compared with other composites, which effectively inhibited further pyrolysis of the polymer matrix, indicating that PDAP had excellent char formation ability for PLA. Combining the previous data analysis and considering the impact on other properties, PLA-4 with 20 wt% addition had more application advantages. Similarly, the degradation of all PLA/PDAP under air atmosphere was earlier than that of PLA, the reason analyzed was that it was closely related to the premature thermal degradation of the IFR system. The overall change in thermal degradation of the materials under Air was essentially the same as under Nitrogen.

### TG-FTIR analysis

With the purpose of obtaining the variation of gas components with temperature of PLA and PLA/PDAP, 3D TG-FTIR spectra of thermal degradation gas products of PLA and PLA-4 were shown in Fig. 6. From the figure, it could be shown that there was no obvious difference between pyrolysis products of pure PLA and PLA-4 during thermal degradation. Absorption bands were found around 3500–3600, 2700–3000, 2100–2400, 1600–1800, 1100–1400 $cm^{-1}$, for example, aldehyde-containing compounds (2740 $cm^{-1}$) and carbonyl compounds (1760 $cm^{-1}$) could be clearly identified [30, 31].

To further investigate the variation of these volatiles with temperature, FTIR spectra of volatile products at different temperatures of PLA and PLA-4 were shown in Fig. 7. From the figure, both PLA and PLA-4 had characteristic absorption bands in water molecules (3575 $cm^{-1}$), methane compounds (2975 $cm^{-1}$, 1373 $cm^{-1}$), aldehydes containing compounds (2740 $cm^{-1}$) and carbonyl compounds (1760 $cm^{-1}$) [32]. The absorption band of $CO_2$ was at 2310 $cm^{-1}$, the absorption band of CO was at 2176, 2108 $cm^{-1}$, and the absorption band of 1120 $cm^{-1}$ was from fatty ether. There was also a characteristic absorption band of $NH_3$ at 930 $cm^{-1}$ in PLA-4 thermal degradation gas shown in Fig. 7(b), and it started to appear at about 360 °C, reached the highest intensity at 384 °C. There was no longer an absorption peak of $NH_3$ at 411 °C, indicating that the ammonia release was over at this time [25, 33]. For pure PLA shown in Fig. 7(a), the thermal degradation rate reached the maximum around 275 °C, when the intensity of the absorption bands of various thermal degradation gases was the highest. At a temperature of about 357 °C, basically only a weak carbonyl compound stretching vibration absorption peak existed, indicating that PLA was going to be totally degraded at this moment. As for the PLA-4 presented in Fig. 7(b), there was only a weak absorption peak at 330 °C, indicating that the generation of composite gas products started at about this temperature. The rate of thermal degradation of PLA-4 achieved the maximum around 384 °C., and basically only the absorption bands of carbonyl compounds were present around 425 °C. Comparing the FTIR spectra of pyrolysis

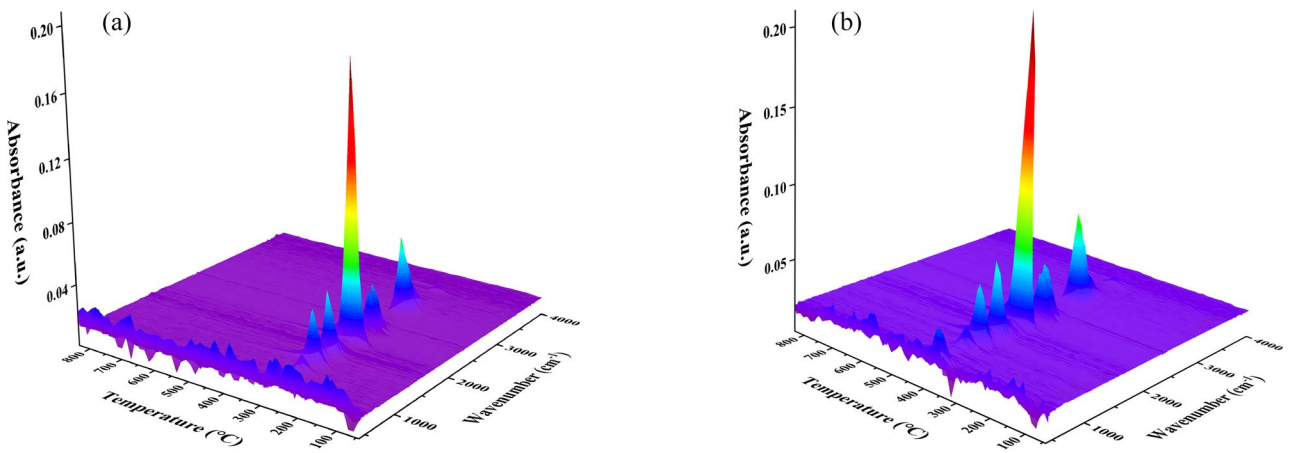


**Fig. 6** 3D TG-FTIR spectra of gas products of pure PLA (**a**) and PLA-4 (**b**)

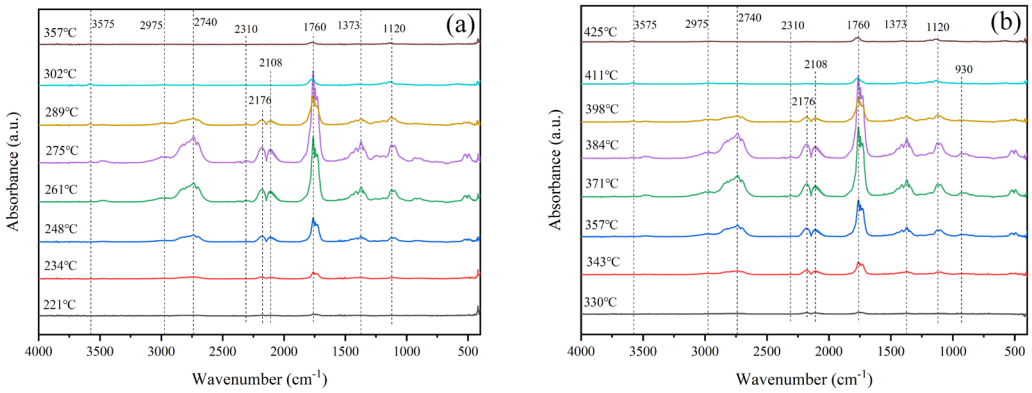


**Fig. 7** FTIR spectra of gas products of pure PLA (**a**) and PLA-4 (**b**) at different temperatures

gas with temperature for PLA and PLA-4, PLA/PDAP produced pyrolysis gas at a higher temperature than pure PLA by about 100 °C. This was mainly explained by the addition of PDAP, which resulted in higher thermal stability of PLA-4, further indicating that PDAP had outstanding flame retardant properties for PLA.

## Analysis of residual char of PLA composites

### FTIR spectra of residual char

As presented in Fig. 8, FTIR spectra of the residual char of PLA/PDAP after CCT test showed absorption bands at 2924 and 2853 $cm^{-1}$ (C-H) and 3429 $cm^{-1}$ (O-H, adsorbed moisture) [34], and the absorption band of -P-0-Si- was at 1180 $cm^{-1}$. Furthermore, the large absorption bands at 1018 and 1154 $cm^{-1}$ corresponded to -Si-O-Si- bonds. 1018, 1103 and 494 $cm^{-1}$ absorption bands were belong to -Si-O-Si /-P-O-C-, -Si-O-C /PO2- and $PO_4$ in $PO_4^{3-}$, which indicated

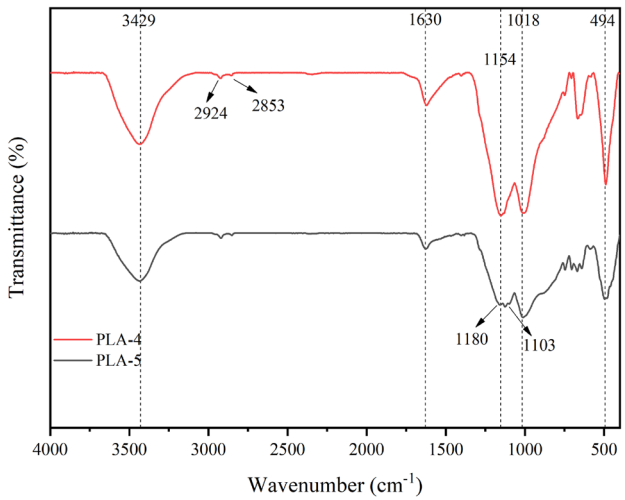


**Fig. 8** FTIR spectra of residual char of PLA-4 and PLA-5

the phosphoric and polyphosphoric acid formation, and the C=O in PLA remained at 1630 $cm^{-1}$. It was because -Si-O-C, -Si-O-Si-, -P-O -Si-, -P-O-C-, and -P-O-P- reinforced completeness and robustness of the char layer, creating a strong barrier against further combustion of the substrate at high temperatures. This suggested that the form of high quality char layer of PLA-4 and PLA-5 could shield the PLA matrix from heat and flammable gas, and eventually induced a greater number of PLA molecules to engage in carbonization [35].

### The picture and SEM-EDS analysis of the residual char

The char residue after CCT was analyzed in both macroscopic and microscopic perspectives. Figure 9 showed digitized pictures of the char residue on PLA and PLA/PDAP tested by CCT, and Fig. 10 showed the microscopic morphology of the residual charcoal at various magnifications. As the amount of PDAP increased, the char layer became more continuous and denser, and then formed a multi-layer char layer. The reason was the good char-forming effect of PDAP and the fact that PDAP emitted a large number of non-combustible and inert gases when combustion process, resulting in the expansion of the char layer, foaming and extrusion of each other, to get a strong, dense, thick char layer. The char layer of PLA-2 had some holes and small bumps although it had a contiguous surface. This was because of the lack of strength of the char layer, which was squeezed by the gas released during combustion process, even forming a distorted surface with a large number of holes. Surfaces of PLA-3, PLA-4 and PLA-5 char layers were continuous, dense and structurally flat. It indicated that the char layer created by the cross-linking reaction among PLA/PDAP decomposition products were structurally stable and high quality char was obtained. It could play a high-strength barrier role by isolating heat and blocking

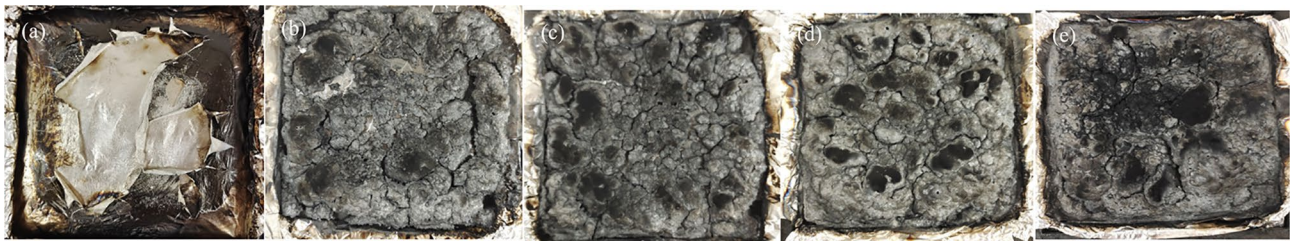


**Fig. 9** The digital picture of residual char after CCT. **a**: pure PLA, **b**: PLA-2, **c**: PLA-3, **d**: PLA-4 and **e**: PLA-5

gas transmission, preventing further pyrolysis of the inner material matrix.

The EDS of PLA-4 composite was shown in the Fig. 10, and it could be noticed that the carbon content was as high as 42.6%, which was due to the good char formation effect of PDAP. The PO• generated by PDAP effectively burst the reactive free radicals and inhibited the pyrolysis of PLA.

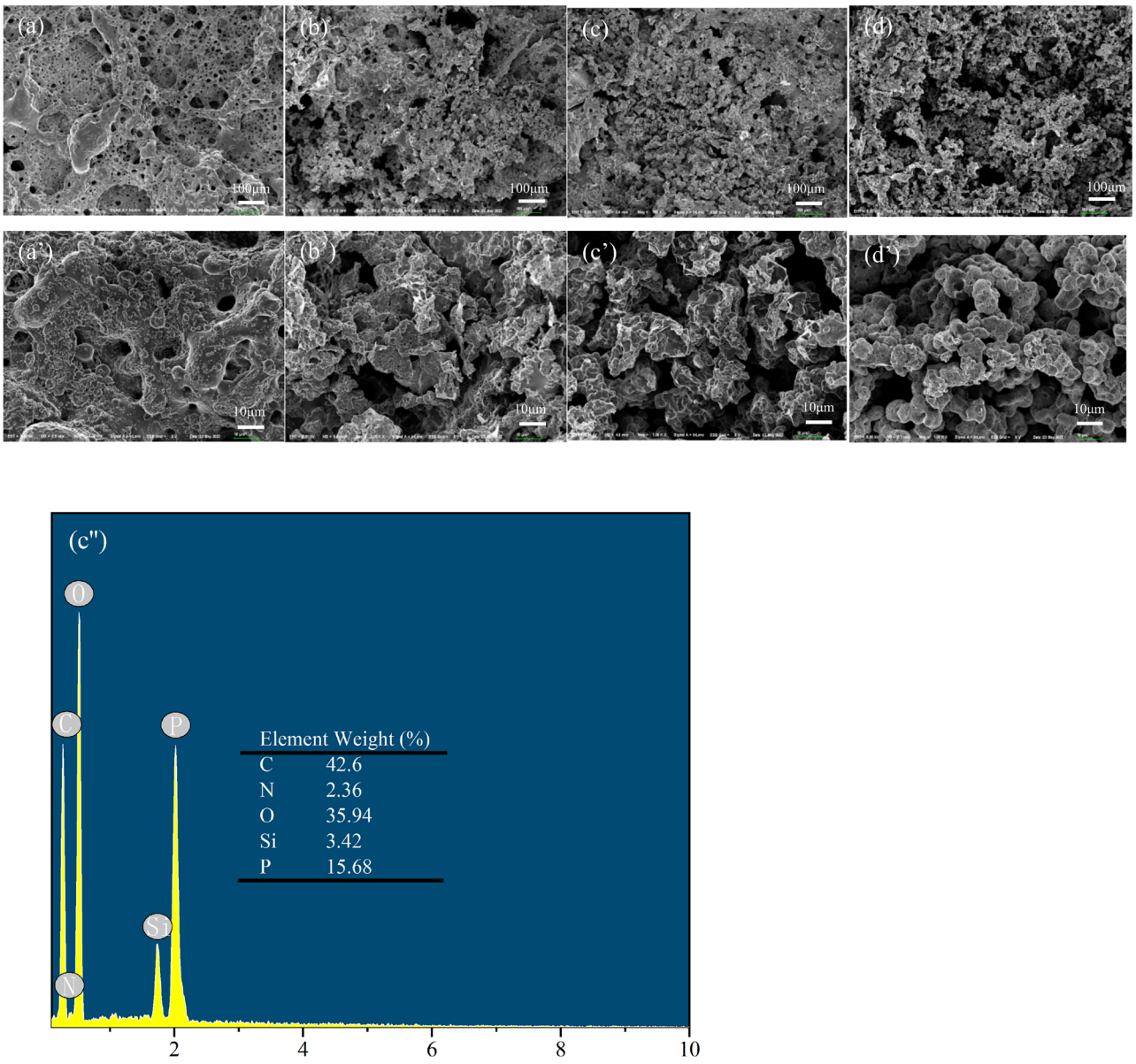


**Fig. 10** SEM micrographs of residual char after CCT and EDS image of PLA-4 residual char, **a**, **a'**: PLA-2, **b**, **b'**: PLA-3, **c**, **c'**, **c''**: PLA-4, **d**, **d'**: PLA-5

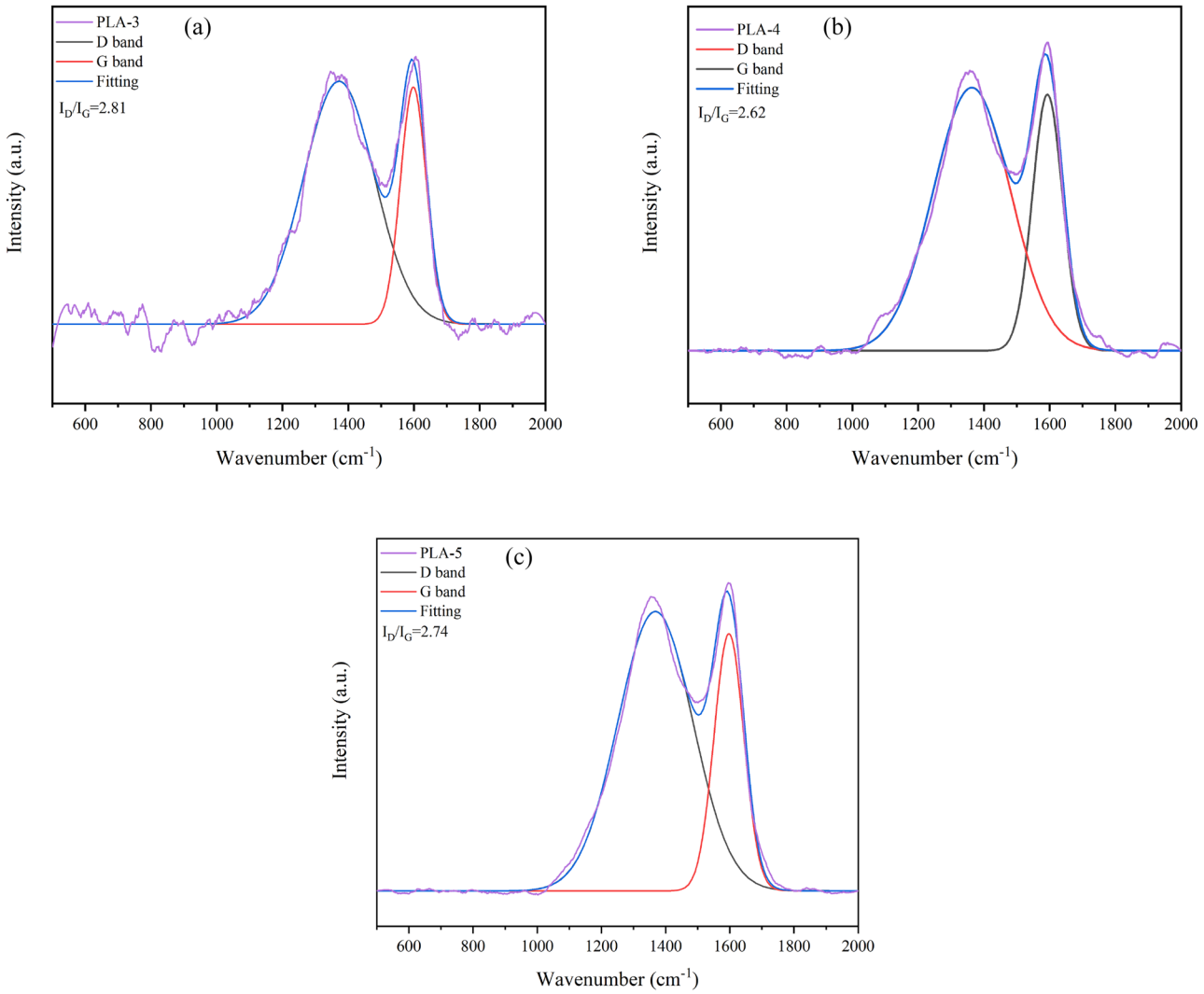


**Fig. 11** LRS of the residual char for PLA-3, PLA-4 and PLA-5

### LRS analysis of residual char

The LRS spectra of residual char after CCT test for PLA/PDAP were presented in Fig. 11. The Raman spectra consists of two overlapping bands located at around 1600 cm-1 (G band, crystalline carbon) and 1360 cm-1 (D band, amorphous carbon). The extent of graphitization of the char residue was indicated by the value of $I_D/I_G$, which is the integral intensity of the D and G bands [36]. The higher the value of $I_D/I_G$, the lower the level of graphitization. Highly graphitized char indicates better thermal stability and barrier properties, which could effectively delay the fire and protect the internal material matrix from further combustion. LRS analysis indicated that the addition of 20 wt% PDAP to the PLA matrix with the lowest $I_D/I_G$ value of 2.62 resulted in the highest graphitization of the composite, which further confirmed that PLA-4 had better char formation ability, giving PLA excellent flame retardant performance, which was consistent with the previous results.

### Possible flame retardant mechanism

The excellent flame retardancy obtained from the test analysis was the result of the interaction between the decomposition products of PDAP and those of the matrix. The possible flame retardant mechanism of PDAP for PLA was presented in Fig. 12. The self-condensation of -Si-OH and P-OH groups facilitated the formation of crosslinked networks, and this cross-linked char layer containing phosphorus-silica had high strength, which kept intact and continuous even under a large amount of gas release and facilitated the condensed phase flame retardant mechanism [26]. PDAP generated radicals containing phosphorus oxides, which included phosphate and pyrophosphate radicals. They could

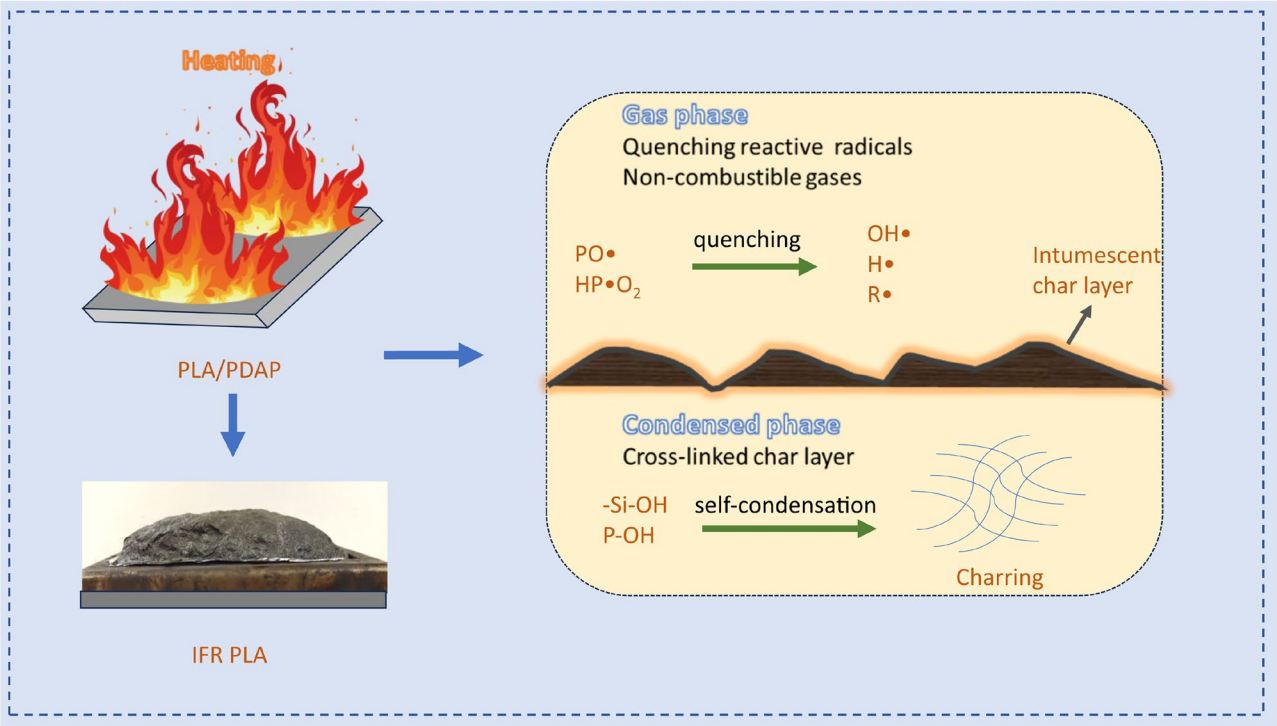


**Fig. 12** Possible flame retardant mechanism of IFR

quench the reactive radicals generated by the decomposition of PLA matrix [7], interrupted the free radical chain reaction during combustion, and remained in the condensed phase as residues. Meanwhile, the non-combustible gas released in the combustion process, including $CO_2$, $NH_3$ and $H_2O$, which not only could dilute the content of combustible gases, but also removed part of the heat, so that the intensity of combustion was reduced and the flame was suppressed, which resulted in a gas-phase flame retardant mechanism. It helped to form an intumescent char layer to cover the substrate material. Continuous dense and thermally stable char layer could isolate the transfer of heat and oxygen effectively and protect the substrate material from more combustion [16, 28]. The Si element had a good synergistic effect with P-system flame retardants. The decomposition of silicone at high temperature produced $Si_2O$ migrating to the polymer surface, which formed a thermally stable surface layer containing silicon and prevented further decomposition of the polymer.

## Conclusion

A single-component IFR PDAP containing nitrogen, phosphorus and silicon was synthesized and added to PLA. When added at 20 wt%, PLA-4 exhibited superior flame retardancy. The LOI value was 37%, which was 84% higher than that of pure PLA, and the UL-94 test could reach V-0 rating, which could solve the problem of easy molten drops when PLA combusts. TG analysis and CCT test showed that PLA composites had high residual char formation rate and low exothermic capacity. Compared with pure PLA with no residue at 800 °C, PLA-4 achieved a residue rate of 11.98% at 800 °C, which effectively protected the internal matrix material. The PHRR of PLA-4 was reduced by 62.1%, the THR by 36.8%, and the Av-EHC by 19.5%. In addition, the microscopic morphology of the residual char could be observed by SEM, PLA-4 showed a dense and continuous char layer, which effectively isolated the thermal mass transfer. The laser Raman spectrogram also showed that PLA-4 formed a thermally stable char layer. The results indicated that this paper synthesizes an efficient flame retardant applicable to PLA.

**Supplementary Information** The online version contains supplementary material available at https://doi.org/10.1007/s10965-023-03805-4.

**Funding** We gratefully acknowledge the financial supports by Supported by Program for New Century Excellent Talents in University (NCET-12–0912).

## Declarations

**Competing interest** The authors declare that they have no known competing financial interests or personal relationships that could have appeared to influence the work reported in this paper.

## References


1. Li C, Ma C, Li J (2020) Highly efficient flame retardant poly(lactic acid) using imidazole phosphate poly(ionic liquid). Polym Adv Technol 31(8):1765–1775. https://doi.org/10.1002/pat.4903
2. Ye G, Huo S, Wang C, Shi Q, Liu Z, Wang H (2021) One-step and green synthesis of a bio-based high-efficiency flame retardant for poly (lactic acid). Polym Degrad Stab 192:109696. https://doi.org/10.1016/j.polymdegradstab.2021.109696
3. Wang X, He W, Long L, Huang S, Qin S, Xu G (2021) A phosphorus- and nitrogen-containing DOPO derivative as flame retardant for polylactic acid (PLA). J Therm Anal Calorim 145(2):331–343. https://doi.org/10.1007/s10973-020-09688-7
4. Zhan Y, Wu X, Wang S, Yuan B, Fang Q, Shang S, Cao C, Chen G (2021) Synthesis of a bio-based flame retardant via a facile strategy and its synergistic effect with ammonium polyphosphate on the flame retardancy of polylactic acid. Polym Degrad Stab 191:109684. https://doi.org/10.1016/j.polymdegradstab.2021.109684
5. Wu N, Yu J, Lang W, Ma X, Yang Y (2019) Flame retardancy and toughness of poly(lactic acid)/GNR/SiAHP composites. Polymers 11(7):1129. https://doi.org/10.3390/polym11071129
6. Yin N, Zhong J, Tian H, Zhou Z, Ying W, Dai J, Li W, Zhang W (2022) Synthesis of P-/N-Containing bamboo-activated Carbon toward enhanced Thermal Stability and Flame Retardancy of Polylactic Acid. Materials 15(19):6802. https://doi.org/10.3390/ma15196802
7. Gong W, Fan M, Luo J, Liang J, Meng X (2021) Effect of nickel phytate on flame retardancy of intumescent flame retardant polylactic acid. Polym Adv Technol 32(4):1548–1559. https://doi.org/10.1002/pat.5190
8. Jin X, Gu X, Chen C, Tang W, Li H, Liu X, Serge B, Zhang Z, Sun J, Zhang S (2017) The Fire performance of polylactic acid containing a novel intumescent flame retardant and intercalated layered double hydroxides. J Mater Sci 52(20):12235–12250. https://doi.org/10.1007/s10853-017-1354-5
9. Wang X, Li Y, Liao W, Gu J, Li D (2008) A new intumescent flame-retardant: preparation, surface modification, and its application in polypropylene. Polym Adv Technol 19(8):1055–1061. https://doi.org/10.1002/pat.1077
10. Qin Y, Li M, Huang T, Shen C, Gao S (2022) A study on the modification of polypropylene by a star-shaped intumescent flame retardant containing phosphorus and nitrogen. Polym Degrad Stab 195:109801. https://doi.org/10.1016/j.polymdegradstab.2021.109801
11. Yang W, Tawiah B, Yu C et al (2018) Manufacturing, mechanical and flame retardant properties of poly(lactic acid) biocomposites based on calcium magnesium phytate and carbon nanotubes. Compos Part A: Appl Sci Manufac 110:227–236. https://doi.org/10.1016/j.compositesa.2018.04.027
12. Zhou L, Liang Z, Li R, Huang D, Ren X (2017) Flame-retardant treatment of cotton fabric with organophosphorus derivative containing nitrogen and silicon. J Therm Anal Calorim 128(2):653–660. https://doi.org/10.1007/s10973-016-5949-x
13. Xia S, Zhang Z, Leng Y, Li B, Xu M (2018) Synthesis of a novel mono-component intumescent flame retardant and its high efficiency for flame retardant polyethylene. J Anal Appl Pyrol 134:632–640. https://doi.org/10.1016/j.jaap.2018.08.017
14. Gao S, Zhao X, Liu G (2017) Synthesis of an integrated intumescent flame retardant and its flame retardancy properties for polypropylene. Polym Degrad Stab 138:106–114. https://doi.org/10.1016/j.polymdegradstab.2016.05.007
15. Qi H, Liu S, Chen X, Shen C, Gao S (2020) The flame retardant and thermal performances of polypropylene with a novel intumescent flame retardant. J Appl Polym Sci 137(36):49047. https://doi.org/10.1002/app.49047
16. Zhu C, He M, Cui J, Tai Q, Song Lei, Hu Y (2018) Synthesis of a novel hyperbranched and phosphorus-containing charring-foaming agent and its application in polypropylene. Polym Adv Technol 29(9):2449–2456. https://doi.org/10.1002/pat.4355
17. Lai X, Tang S, Li H, Zeng X (2015) Flame-retardant mechanism of a novel polymeric intumescent flame retardant containing caged bicyclic phosphate for polypropylene. Polym Degrad Stab 113:22–31. https://doi.org/10.1016/j.polymdegradstab.2015.01.009
18. Li Q, Jiang P, Wei P (2005) Studies on the properties of polypropylene with a new silicon-containing intumescent flame retardant. J Polym Sci Part B: Polym Phys 43(18):2548–2556. https://doi.org/10.1002/polb.20545
19. Fang M, Qian J, Wang X, Chen Z, Guo R, Shi Y (2021) Synthesis of a Novel Flame Retardant containing Phosphorus, Nitrogen, and Silicon and its application in Epoxy Resin. ACS Omega 6(10):7094–7105. https://doi.org/10.1021/acsomega.1c00076
20. Song K, Wang Y, Ruan F, Yang W, Liu J (2020) Synthesis of a Novel Spirocyclic Inflatable Flame Retardant and its application in Epoxy composites. Polymers 12(11):2534. https://doi.org/10.3390/polym12112534
21. Kong D, Liu J, Zhang Z, Wang S, Zhou L (2021) Preparation of synergistic silicon, phosphorus and nitrogen flame retardant based on cyclosiloxane and its application to cotton fabric. Cellulose 28(12):8115–8128. https://doi.org/10.1007/s10570-021-04019-x
22. Liu J, Dong C, Zhang Z, Sun H, Kong D, Lu Z (2020) Durable flame retardant cotton fabrics modified with a novel silicon–phosphorus–nitrogen synergistic flame retardant. Cellulose 27(15):9027–9043. https://doi.org/10.1007/s10570-020-03370-9
23. Wang M, Yu T, Feng Z, Sun J, Gu X, Li H, Fei B, Zhang S (2020) Preparation of 3-aminopropyltriethoxy silane modified cellulose microcrystalline and their applications as flame retardant and reinforcing agents in epoxy resin. Polym Adv Technol 31(6):1340–1348. https://doi.org/10.1002/pat.4863
24. Duan R, Wu H, Li J, Zhou Z, Meng W, Liu L, Qu H, Xu J (2022) Phosphor Nitrile functionalized UiO-66-NH2/graphene hybrid flame retardants for Fire safety of epoxy. Colloids Surf a 635:128093. https://doi.org/10.1016/j.colsurfa.2021.128093
25. Wang S, Du Z, Cheng X, Liu Y, Wang H (2018) Synthesis of a phosphorus- and nitrogen-containing flame retardant and evaluation of its application in waterborne polyurethane. J Appl Polym Sci 135(16):46093. https://doi.org/10.1002/app.46093
26. Zhao Z, Jin Q, Zhang N, Guo X, Yan H (2018) Preparation of a novel polysiloxane and its synergistic effect with ammonium polyphosphate on the flame retardancy of polypropylene. Polym Degrad Stab 150:73–85. https://doi.org/10.1016/j.polymdegradstab.2018.02.007
27. Chen X, Zhuo J, Jiao C (2012) Thermal degradation characteristics of flame retardant polylactide using TG-IR. Polym Degrad Stab 97(11):2143–2147. https://doi.org/10.1016/j.polymdegradstab.2012.08.016
28. Yang R, Ma B, Zhang X, Li J (2019) Fire retardance and smoke suppression of polypropylene with a macromolecular intumescent flame retardant containing caged bicyclic phosphate and piperazine. J Appl Polym Sci 136(25):47593. https://doi.org/10.1002/app.47593
29. Duan L, Yang H, Song L, Hou Y, Wang W, Gui Z, Hu Y (2016) Hyperbranched phosphorus/nitrogen-containing polymer in combination with ammonium polyphosphate as a novel flame retardant system for polypropylene. Polym Degrad Stab 134:179–185. https://doi.org/10.1016/j.polymdegradstab.2016.10.004
30. Bao DM, Wang JH, Hou ZM, Xu ZY, Ye XL, Qi YZ, Xu SJ, Long LJ, Wu ZL, Wen Z (2022) Synthesis of a novel flame retardant with phosphaphenanthrene and phosphazene double functional groups and flame retardancy of poly (lactic acid) composites. Front Mater 9:951515. https://doi.org/10.3389/fmats.2022.951515

31. Tang G, Zhang R, Wang X, Wang B, Song L, Hu Y, Gong X (2013) Enhancement of Flame Retardant performance of Bio-based Polylactic Acid composites with the Incorporation of Aluminum Hypophosphite and expanded graphite. J Macromolecular Sci Part A 50(2):255–269. https://doi.org/10.1080/10601325.2013.742835
32. Yi C, Xu C, Sun N et al (2023) Flame-retardant and transparent poly(methyl methacrylate) composites based on Phosphorus–Nitrogen Flame retardants. ACS Appl Polym Mater 5(1):846–855. https://doi.org/10.1021/acsapm.2c01786
33. Wang B, Li J, Lai X et al (2021) Synthesis of a novel N -alkoxyamine containing macromolecular intumescent flame retardant and its synergism in flame-retarding polypropylene. Polym Adv Technol 32(6):2452–2464. https://doi.org/10.1002/pat.5275
34. Makhlouf G, Abdelkhalik A, Hassan MA (2020) Combustion toxicity of polypropylene containing melamine salt of pentaerythritol phosphate with high efficiency and stable flame retardancy performance. Process Saf Environ Prot 138:300–311. https://doi.org/10.1016/j.psep.2020.04.012
35. Yang W, Zhang H, Hu X et al (2021) Self-assembled bio-derived microporous nanosheet from phytic acid as efficient intumescent flame retardant for polylactide. Polym Degrad Stab 191:109664. https://doi.org/10.1016/j.polymdegradstab.2021.109664
36. Xu W, Wang S, Li A, Wang X (2016) Synthesis of aminopropyltriethoxysilane grafted/tripolyphosphate intercalated ZnAl LDHs and their performance in the flame retardancy and smoke suppression of polyurethane elastomer. RSC Adv 6(53):48189–48198. https://doi.org/10.1039/c6ra06713a